Neuropharmacology xxx (2014) 1–13

Contents lists available at ScienceDirect

Neuropharmacology

journal homepage: www.elsevier.com/locate/neuropharm

Mode of action of the positive modulator PNU-120596 on α7 nicotinic acetylcholine receptors

Anett K. Szabo [a,b], Krisztina Pesti [a,b], Arpad Mike [b,*], E. Sylvester Vizi [b]

[a] Semmelweis University, School of Ph.D. Studies, Üllői út 26, H-1085 Budapest, Hungary
[b] Laboratory of Molecular Pharmacology, Institute of Experimental Medicine, Hungarian Academy of Sciences, P.O.B. 67, H-1450 Budapest, Hungary

ARTICLE INFO

Article history:
Received 23 March 2013
Received in revised form
13 January 2014
Accepted 21 January 2014

Keywords:
α7 nicotinic acetylcholine receptor
Choline
PNU-120596
Positive allosteric modulator
Mode of action

ABSTRACT

We investigated the mode of action of PNU-120596, a type II positive allosteric modulator of the rat α7 nicotinic acetylcholine receptor expressed by GH4C1 cells, using patch-clamp and fast solution exchange. We made two important observations: first, while PNU-120596 rapidly associated to desensitized receptors, it had at least hundredfold lower affinity to resting conformation, therefore at 10 μM conformation it dissociated from resting receptors; and second, binding of PNU-120596 slowed down dissociation of choline molecules from the receptor radically. We propose that when agonist concentration is transiently elevated in the continuous presence of the modulator (as upon the neuronal release of acetylcholine in a modulator-treated animal) these two elements together cause occurrence of a cycle of events: Binding of the modulator is limited in the absence of the agonist. When the agonist is released, it binds to the receptor, and induces desensitization, thereby enabling modulator binding. Modulator binding in turn traps the agonist within its binding site for a prolonged period of time. Once the agonist finally dissociated, the modulator can also dissociate without re-binding, and the receptor assumes its original resting conformation. In kinetic simulations this "trapped agonist cycle" mechanism did not require that the orthosteric and allosteric ligands symmetrically modify each other's affinity, only the modulator must decrease agonist accessibility, and the agonist must induce a conformation that is accessible to the modulator. This mechanism effectively prolongs and amplifies the effect of the agonist.

1. Introduction

The α7 subunit containing subtype of nicotinic acetylcholine receptor (α7 nAChR) is abundant in the CNS, and also present in many non-neural tissues. It is involved in the regulation of growth and differentiation in general, and in synaptic plasticity in particular. Pro-cognitive, anti-ischemic, anti-inflammatory, and anti-nociceptive effects of its agonists and positive allosteric modulators (PAMs) make this receptor a promising target in a number of disorders including Alzheimer's disease, schizophrenia, Parkinson's disease, chronic pain, inflammatory diseases and even myocardial infarction (AhnAllen, 2012; Costa et al., 2012; Freitas et al., 2013; Isaacson et al., 2013; Li et al., 2013; Liu and Su, 2012; Mazurov et al., 2012; Russo and Taly, 2012; Vizi et al., 2010; Williams et al., 2011b; Xiong et al., 2012).

Agonists and positive allosteric modulators (PAMs) of the α7 nAChR are prospective pro-cognitive drugs in different types of dementia, and in schizophrenia. Several pre-clinical and clinical studies have demonstrated their effectiveness (AhnAllen, 2012; Faghih et al., 2007, 2008; Mazurov et al., 2012; Williams et al., 2011b). Two major classes of PAMs are known (Gronlien et al., 2007; Williams et al., 2011b): type I PAMs increase the amplitude of currents, but do not significantly modify their kinetics, while type II PAMs profoundly change the kinetics of currents, by radically prolonging single channel open times. The advantage of PAMs over agonists is that the physiological spatio-temporal pattern of neuronal activation is preserved; the modulators only augment α7 nAChR-mediated signals. This pharmacological approach has been proven to be successful in the case of $GABA_A$ receptors (benzodiazepines and barbiturates). In the case of α7 nAChRs, however, much less is known about the mode of action of PAMs, and most PAM compounds have only been developed recently. One of the most studied type II PAMs is the compound PNU-120596. The last few years brought some impressive results regarding the mode of action of PNU-120596, such as the effect of the drug on the single channel behavior of the receptor (daCosta et al., 2011; Williams et al., 2011a), the state-dependence of PNU-120596 effect

Abbreviations: α7 nAChR, α7 subtype nicotinic acetylcholine receptor; PNU-120596, 1-(5-chloro-2,4-dimethoxyphenyl)-3-(5-methylisoxazol-3-yl)urea; PAM, positive allosteric modulator; SXT, 10–90% solution exchange time; AUC, area under curve.

* Corresponding author. Tel.: +36 12109971; fax: +36 12109423.
E-mail address: mike@koki.hu (A. Mike).

0028-3908/$ – see front matter © 2014 Published by Elsevier Ltd.
http://dx.doi.org/10.1016/j.neuropharm.2014.01.033

(Isaacson et al., 2013; Wang et al., 2012; Williams et al., 2011a), and the temperature-dependence of both receptor gating, and PNU-120596 action(Jindrichova et al., 2012; Sitzia et al., 2011; Williams et al., 2012). Nevertheless, some very basic aspects of the effect of PNU-120596 on receptor function are still not fully understood (Bouzat et al., 2008; daCosta et al., 2011; Papke et al., 2009; Williams et al., 2011a,b). We investigated the following specific questions: What is the mechanism behind the distinctive biphasic curve observed when agonists are applied in the presence of PNU-120596 (Gronlien et al., 2007; Malysz et al., 2009b)? Is there a difference in the affinity of PNU-120596 to different conformational states of the receptor? The receptor has been shown to have distinct desensitized states, which have different sensitivity to PNU-120596 (Papke et al., 2009; Uteshev et al., 2002; Wang et al., 2012; Williams et al., 2011a). Can we detect this difference? Can the modulator bind to the resting receptor? How can the effect of PNU-120596 be explained in terms of influencing conformational transition rates? Does it increase the affinity of the agonist? The possible cooperativity between agonist and PAM is controversial (daCosta et al., 2011; Williams et al., 2011b). An apparent increase in agonist affinity is obvious (Hurst et al., 2005), but it must be understood that agonist-evoked current amplitudes misrepresent concentrations because the rate of solution exchange is insufficient as compared to the fast gating of the channel (Papke et al., 2000; Papke and Thinschmidt, 1998). Slowing down current kinetics would inevitably cause an increase of apparent affinity, therefore it is not clear whether type II PAMs indeed induce a conformational change of the orthosteric site that increases its affinity, or rather they only reveal its true affinity by slowing gating kinetics. Finally, the opposite interaction is also unsettled: whether the agonist has an effect on the affinity of the PAM binding site, i.e., whether the cooperativity between agonist and PAM must inevitably be mutual?

Our aim was to extend the kinetic model of agonist action on α7 nAChR described in the accompanying paper (Pesti et al.) by incorporating PNU-120596-bound states as well, in the hope that our attempt to reproduce experimentally observed phenomena may give an insight into possible mechanisms involved in the action of PNU-120596 on α7 nAChRs.

2. Materials and methods

2.1. Materials

PNU-120596 was obtained from Tocris Bioscience (Bristol, UK). Cell culture products were obtained from Life Technologies™. All other chemicals were obtained from Sigma.

2.2. Cell culture

GH4C1 cells stably transfected with pCEP4/rat α7 nAChR were obtained from Siena Biotech S.p.A. (Siena, Italy). Cells were cultured in poly-L-lysine coated Petri dishes using HAM's F10 medium supplemented with 15% horse serum, 2.5% foetal bovine serum, 1% penicillin–streptomycin, 1 mM GlutaMAX, 100 μg/ml Hygromycin B.

2.3. Electrophysiology

Electrophysiological recordings were done as described in the accompanying paper (Pesti et al.). Briefly, an Axopatch 200B amplifier and the pCLamp software were used to acquire whole-cell or outside-out patch currents at a holding potential of −70 mV. Currents were digitized at 20 kHz and filtered at 10 kHz; for illustration purposes some of the traces were off-line filtered digitally at 2 kHz. The composition of pipette solution was (in mM): CsCl 55, CsF 65, EGTA 10, HEPES 10 (pH = 7.2), the extracellular solution contained (in mM): NaCl 140, KCl 5 $CaCl_2$ 2, $MgCl_2$ 1, Glucose 5, and HEPES 5 (pH = 7.3). Solution exchange was performed by the "liquid filament switch" method as described in the accompanying paper (Pesti et al.). Briefly: theta glass tubes (1.5 mm O.D.) were pulled to have a tip diameter between 150 and 250 μm and Microfil™ capillary (0.35 mm OD) was inserted into both sides. The solution reservoirs were connected to the pressure control unit of a DAD-12 solution exchange system (ALA Scientific Instruments Inc., Farmingdale, NY), this allowed optimization of flow velocity (typically 5–20 cm/s). Translational velocity was 1–5 cm/s. Voltage command waveforms for the piezoelectric actuator (Burleigh LSS-3200 system) were written in the pCLamp software. Ten to ninety % solution exchange times (SXTs) for individual measurements were determined using open-tip junction potential measurement right after the experiments, without moving the pipette; the values were between 0.5 and 2 ms. Time constants of the removal of channel block confirmed that solution exchange was not significantly delayed by cell geometry or unstirred layer effect.

2.4. Simulations

The simulation was based on a set of differential equations with the occupancy of each receptor state (i.e., the fraction of the receptor population in that specific state) given by the following equation

$$\frac{dS_i(t)}{dt} = \sum_j^n (S_j(t)*k_{ji} - S_i(t)*k_{ij})$$

where $S_i(t)$ is the occupancy of a specific state at the time t, $S_j(t)$ is the occupancy of a neighboring state, n is the number of neighboring states, and k_{ij} and k_{ji} are the rate constants of transitions between neighboring states. Simulations were performed using Berkeley Madonna v8.0.1 (www.berkeleymadonna.com), or QuB (www.qub.buffalo.edu) (Milescu et al., 2000–2013).

2.5. Analysis of data

Monoexponential fitting: $I(t) = (I_{max} - I_{min})*\exp(-t/\tau) + I_{min}$ was performed by the Solver function of Microsoft Excel. Paired Student's t test was used for statistical analysis, unless otherwise mentioned. A probability level of 0.05 or less was considered to reflect a statistically significant difference.

3. Results and discussion

3.1. Effect of PNU-120596 on choline-evoked currents

3.1.1. The biphasic nature of PNU-120596-modulated choline-evoked currents

Co-application of 10 mM choline and 10 μM PNU-120596 produced a characteristic biphasic curve with an initial fast peak and a subsequent prolonged activation. The biphasic nature of agonist evoked currents in the presence of PNU-120596 has been observed before (Gronlien et al., 2007; Malysz et al., 2009a), but the physical processes which underlie the two phases of the response have not been identified (Williams et al., 2011b). (We should mention that prolonged co-application of PNU-120596 and ACh also produced a biphasic pattern (Williams et al., 2011a), however, that is an entirely different phenomenon, first because the amplitudes of the two components are similar, and second because it occurs on the time scale of minutes, not milliseconds.) It is important to note that we applied the mixture of agonist and modulator at a 10–90% solution exchange time (SXT) in the range of 0.5–2 ms, therefore the initial part of the evoked current was better resolved. We made the following observations: (i) while it was previously found that the two phases merge at high PNU-120596 concentration (Gronlien et al., 2007 – Fig. 2, Malysz et al., 2009a – Fig. 1, Malysz et al., 2009b – Fig. 8; reviewed in Williams et al., 2011b), they were clearly separated in our experiments even at 10 μM PNU-120596 (and 10 mM choline). The first phase decayed to 14.0 ± 5.5% (n = 10) of the peak, before the rise due to the "secondary component" could be detected (Fig. 1). (ii) The amplitude, as well as

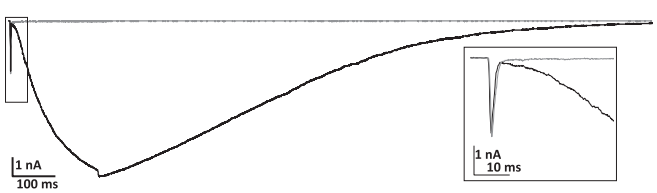

Fig. 1. Co-application of 10 mM choline and 10 μM PNU 120596 (black traces) using submillisecond solution exchange. Inset shows the fast component at an expanded time scale. Gray traces show 10 mM choline application for comparing the fast component to the choline-evoked current.

Please cite this article in press as: Szabo, A.K., et al., Mode of action of the positive modulator PNU-120596 on α7 nicotinic acetylcholine receptors, Neuropharmacology (2014), http://dx.doi.org/10.1016/j.neuropharm.2014.01.033

the rise and decay kinetics of the first component was identical with the current evoked by 10 mM choline alone (Fig. 1), *i.e.*, the rise time was 0.39 ± 0.03 ms, and the decay time constant was 1.01 ± 0.13 ms. We assume that the onset rates for the effect of the agonist choline and the modulator PNU-120596 differ, and using a fast solution exchange, this difference can be resolved. Thus, the first component reflects a pure choline-evoked current unaffected by PNU-120596, and only during the later phase of the decay does the effect of PNU-120596 begin to occur (the second component takes several tens of milliseconds to fully develop). We suppose that the rate limiting step for the first component must be solution exchange rate. For the second component, the onset rate is known to be dependent on PNU-120596 concentration (Gronlien et al., 2007; Malysz et al., 2009b), but it is not clear which exact processes are the major determinants of onset kinetics at high modulator concentration. It may be partitioning of PNU-120596 into the membrane phase (being a lipophilic molecule, and probably having its binding site within the transmembrane domain of the receptor (daCosta et al., 2011; Young et al., 2008), PNU-120596 probably accesses it from the membrane phase), but the binding reaction itself, or any of the gating transitions might also limit onset rate (this question is addressed below in Section 3.2.2). Note that not only a low opening rate can limit the time constant of onset, but any other gating rate involved in the process of activation (e.g., closing, desensitization), by affecting the rate of reaching a gating equilibrium. Slower onset at lower PNU-120596 concentrations is probably limited by concentration-dependent processes, such as partitioning and binding.

3.1.2. Characterization of PNU-120596-modulated choline-evoked currents

Because the first phase was identical with the current evoked by choline alone, the positive modulator effect of PNU-120596 could be assessed within a single biphasic trace. The modulator caused a 14.5 ± 2.4 fold increase in amplitude ($n = 22$; range: 3.3–47.9-fold; median: 10.48-fold). In order to minimize series resistance error, cells and patches, where the choline-evoked current amplitude was higher than 200 pA were excluded from this calculation. The potentiation is somewhat larger than in the original paper that first characterized the effect of PNU-120596 (Hurst et al., 2005), but we used 10 μM PNU-120596 instead of 1 μM. On the other hand, the effect we observed was less than the one described in other publications (Friis et al., 2009; Young et al., 2008). One of the reasons for this may be that we used supramaximal choline concentration, while potentiation is largest at low agonist concentrations. Furthermore, in our experiments the responses to 10 mM choline are fairly well resolved due to the fast solution exchange. Slower solution exchange rates seriously decrease the amplitude of fast choline-evoked currents, but do not affect the slow-onset currents evoked by choline in the presence of PNU-120596; therefore the potentiation seems larger with slower solution exchange.

We observed a characteristic current component at the end of PNU-120596 and 10 mM choline co-application (Figs. 1–4). A rebound current, which was 14.06 ± 2.45% of the PNU-120596-potentiated current in magnitude, appeared with a time constant of 1.37 ± 0.19 ms (this value was close to the solution exchange rates we usually worked with, therefore the true onset kinetics of this component could be even faster). The rebound current was smaller (6.38 ± 1.05%) when the concentration of choline co-applied with 10 μM PNU-120596 was 1 mM, and it was undetectable at 100 μM choline, although the PNU-120596-potentiated current was similar in amplitude within the range of 100 μM–10 mM choline concentration (which means that for 100 μM choline-evoked currents the potentiation is much larger). The rebound current was also absent when co-application of 10 mM choline and 10 μM PNU-120596 was terminated by continuing perfusion of 10 mM choline only (see Section 3.1.3). These observations suggest that the rebound current was at least mostly due to removal of channel block by choline molecules. In single channel recordings, an immediate drop of single-channel noise was observed by Williams et al. (2011a) upon removal of the agonist. Although the single channel amplitude was not increased, an apparent increase can be observed either if the traces are low-pass-filtered at frequency lower than 10 kHz, or if activity of several channels is recorded at the same time. We believe that the rebound current we observed is the multi-channel equivalent of this drop in noise in single-channel recordings.

3.1.3. Dissociation of choline and PNU-120596

We compared the decay after PNU-120596 and choline co-application in three cases: i) When both the agonist and the modulator were removed, ii) When the modulator was removed while agonist perfusion continued, and iii) when the agonist was removed while the modulator was still present. Examples for individual traces as well as the averaged results of 15 -15 traces from each of the three protocols are shown in Fig. 2. As we have mentioned, the rebound component could only be seen when choline was removed. Fitting the decay phases with the single exponential function gave time constants 293.9 ± 12.3 ms, 426.6 ± 29.9 ms, and 2372 ± 726.5 ms for full washout, PNU-120596-removed-choline-present, and choline-removed-PNU-120596-present scenarios, respectively ($n = 6$ cells, using the averages of 7–15 individual traces of all three protocols in each cell; all three groups were significantly different from each other). In the presence of PNU-120596 the current did not decay to baseline within the 2.5 s of modulator application. At the end of this 2.5 s period, when the modulator was also removed, the decay had a time constant of 317.9 ± 20.0 ms (not significantly different from the decay rate during full washout). The most striking phenomenon was the prominent deceleration of decay in the presence of PNU-120596 alone ($p < 0.001$, $n = 6$). Because PNU-120596 in itself cannot cause activation of the receptor, we need to suppose that choline must have been kept bound to the receptor throughout the slow decay, and the decay rate primarily reflects the rate of choline dissociation. The phenomenon has recently been studied on the level of single receptor-mediated currents, where currents persisted for 2.57 ± 0.2 s after removal of the agonist (Williams et al., 2011a), which is very similar to the time constant we observed. The decreased rate of choline dissociation may imply that PNU-120596 binding radically increases the affinity of choline to the receptor, but it is also possible that the effect is on the accessibility, not the affinity of the orthosteric binding site (i.e., both access and egress rates are reduced as a consequence of PNU-120596 binding). As for the decay in the presence of choline alone, it must, in contrast, reflect the dissociation rate of PNU-120596. The time constant was somewhat higher than at full washout ($p < 0.01$, $n = 6$), but the small difference indicates that dissociation of the modulator was not strongly delayed by bound agonist molecules. The mutual cooperativity, which is predicted by the allosteric theory (see (Williams et al., 2011b) for discussion) did not seem to be symmetrical: While PNU-120596 caused a radical decrease in the rate of choline dissociation, choline had no such effect, it rather seemed to interact with PNU-120596 binding primarily by inducing desensitized conformation of the receptor, which promoted PNU-120596 association (for the state-dependence of association see also Section 3.1.4.).

3.1.4. Association of PNU-120596 to resting state

In order to understand the mechanism of PNU-120596 action on α7 nAChRs, we need to know if PNU-120596 has a preference toward certain states.

Please cite this article in press as: Szabo, A.K., et al., Mode of action of the positive modulator PNU-120596 on α7 nicotinic acetylcholine receptors, Neuropharmacology (2014), http://dx.doi.org/10.1016/j.neuropharm.2014.01.033

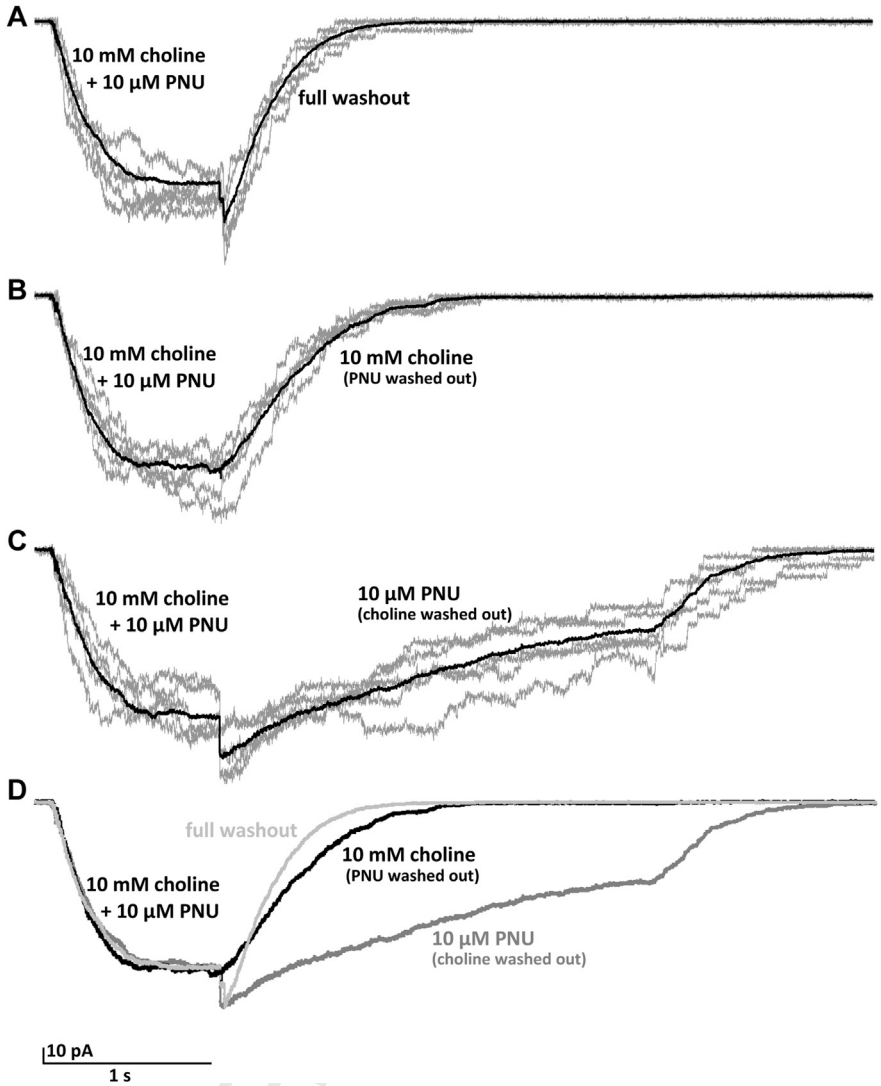

Fig. 2. The decay after 10 mM choline and 10 μM PNU-120596 co-application **(A)** Full washout, **(B)** washout of PNU-120596, and **(C)** washout of choline. Gray lines show five individual traces, Black lines show the average of 15 traces. **(D)** The average traces plotted on the same figure: full washout (light gray), washout of PNU-120596 (black) and washout of choline (dark gray).

Let us consider a simple triangular scheme of resting, open and desensitized receptor (see Scheme 2 in the accompanying paper (Pesti et al.)), and draw a parallel triangle of PNU-120596-bound states (only a single agonist occupancy level is shown, where "n" of the five binding sites are occupied), similarly to the scheme (Fig. 7) shown in the work of daCosta et al. (2011): (Scheme 1) where "p" indicates PNU-120596-bound states. For the sake of simplicity, we do not consider different modulator occupancy levels (monoliganded, diliganded, etc; the receptor probably has five PNU-120596 binding sites), only bound and unbound states. Since we used supramaximal PNU-120596 concentration, we suppose that the majority of binding sites were occupied in the presence of the drug.

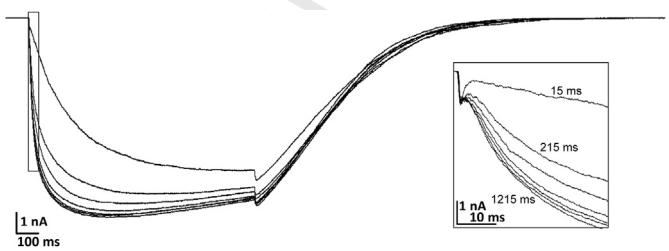

Fig. 3. Pre-incubation with 10 μM PNU 120596 did not significantly decrease the amplitude of the first current phase. A family of currents evoked by co-application of 10 mM choline and 10 μM PNU-120596, after different durations of PNU-120596 pre-incubation: 15, 215, 415, 615, 815, 1015, and 1215 ms. Inset shows the first phase at an expanded time scale.

We aimed to determine, to which of the three states we can assume substantial PNU-120596 association. Association to resting state (a_nR) can be tested by pre-application of PNU-120596. If association to a_nR is possible, then during PNU-120596 application a significant fraction of the receptors will bind the modulator, and be accumulated in pa_nR state. When receptors are in the pa_nR state, the characteristic rapid agonist-induced activation of PNU-120596-unbound receptors (a_nR to a_nO) is impossible, because the current rise time is determined by the gating rate constants (opening rate, closing rate, desensitization rate, etc.) which are drastically slowed down by PNU-120596 binding. Therefore, if a significant fraction of the receptors are in pa_nR state, the first rapid component of the

Please cite this article in press as: Szabo, A.K., et al., Mode of action of the positive modulator PNU-120596 on α7 nicotinic acetylcholine receptors, Neuropharmacology (2014), http://dx.doi.org/10.1016/j.neuropharm.2014.01.033

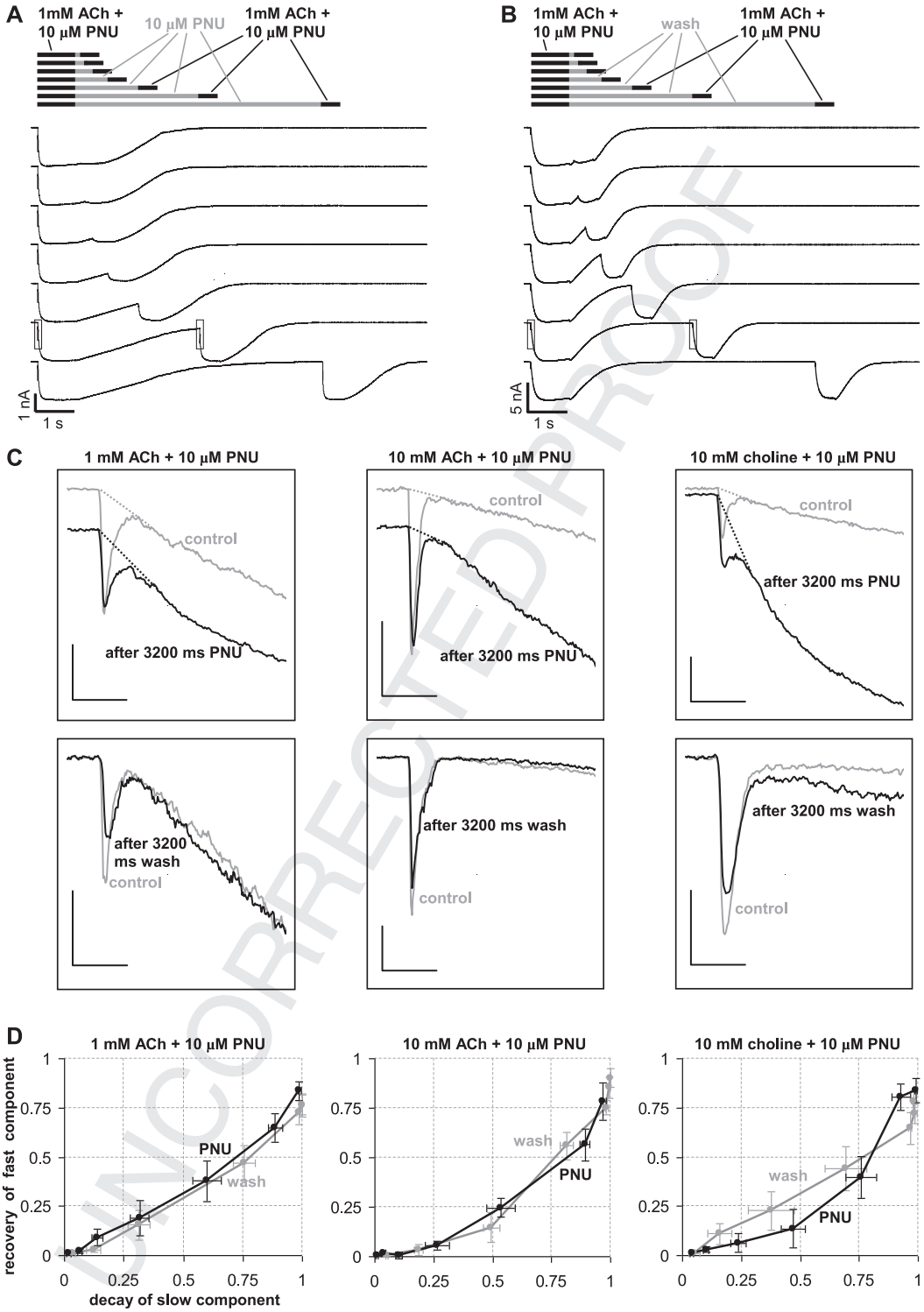

Fig. 4. Re-application of agonists. **(A)** Re-application after 10 μM PNU-120596 perfusion. Boxed areas are shown overlayed in the upper left panel of (C). **(B)** Re-application after washout. Boxed areas are shown overlayed in the lower left panel of (C). **(C)** Examples for currents evoked by the first (gray line) and second (black line) pulse of agonists, after 3200 ms perfusion of either 10 μM PNU-120596 (upper panel), or control extracellular solution (lower panel). Only the initial part is shown, to allow comparison of fast current components. **(D)** The recovery of the fast current component plotted against the decay of the slow current component (agonist-and-modulator-induced activity). Average and SEM values from $n = 5$ or 6 individual cells. On the x axis zero indicates full relative amplitude, while 1 indicates fully decayed slow current component. Decay of the slow component indicates partial or full dissociation of ligands and transition into one of the non-conducting states. Recovery of the fast component, on the other hand, indicates the ratio of fully unbound and recovered receptors. The latter lags behind the former, as shown by the extent of deviation from the diagonal.

Please cite this article in press as: Szabo, A.K., et al., Mode of action of the positive modulator PNU-120596 on α7 nicotinic acetylcholine receptors, Neuropharmacology (2014), http://dx.doi.org/10.1016/j.neuropharm.2014.01.033

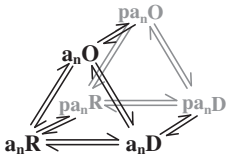

Scheme 1. Three-state model of the α7 nAChR with PNU-120596-bound states.

current must be significantly decreased. The predominant route for this mechanism is illustrated in Scheme 2.

However, what we found in PNU-120596 pre-application experiments was just the opposite. A typical recording is shown in Fig. 3, with currents evoked after pre-application times 15, 215, 415, 615, 815, 1015, and 1215 ms. Pre-application of PNU-120596 left the first current phase essentially unchanged (a non-significant 9.4 ± 5.0% decrease was observed; $n = 5$), while the second phase was significantly accelerated. With the shortest, 15 ms PNU-120596 pre-application (for technical reasons we could not use 0 ms pre-application) the onset of the second phase occurred with a time constant of 115.1 ± 41.1 ms (monoexponential fitting; range: 30.6–286 ms). After 615 ms of PNU-120596 pre-application the onset of the second phase was accelerated, and could no more be fitted with a monoexponential function. A fast time constant of 10.7 ± 2.3 ms appeared, which constituted 54.9 ± 5.8% of the amplitude, and the slow time constant was also accelerated: it was 53.3 ± 19% ms (range: 21.9–139 ms). Although the cell-to-cell variance in the time constants of onset was considerable, the acceleration was evident in all cases, and even the slow time constant was significantly shorter (2.18 ± 0.38 fold difference; $p < 0.05$, $n = 5$) after 615 ms pre-application than after 15 ms pre-application. Longer pre-applications (up to 80 s) did not further accelerate the second phase of activation, and did not further decrease the amplitude of the first current phase. After 80 s of pre-incubation the first phase amplitude was still unchanged (we observed a non-significant 5.1 ± 4.3% decrease; $n = 5$).

We propose therefore, that the predominant route traveled by the receptors is via desensitized states, as illustrated in Scheme 3.

What can be the mechanism of acceleration, if we suppose that it is not due to association of PNU-120596 to its binding site? We know that the binding site of PNU-120596 is within the transmembrane domain of the receptor, and we also know that the molecule is lipophilic (its calculated log*P* value is 2.57). We propose that PNU-120596 might access its binding site from the membrane phase. Partitioning into, and accumulation within the membrane may be the process that requires a few hundred milliseconds. Once the equilibrium of partitioning has been reached and the membrane phase is saturated, binding can occur at a higher rate.

The partial merging of the two components seen upon prolonged PNU-120596 pre-application (Fig. 3) is not likely to be due to direct association to open channels (a$_n$O to pa$_n$O transition). Because the dwell time in a$_n$O is extremely short (less than 100 μs (daCosta et al., 2011; Williams et al., 2011a)) and the open probability is extremely low, it is unlikely that a significant fraction of PNU-120596 association would occur to open receptors.

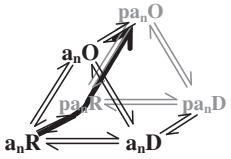

Scheme 2. Hypothetical predominant pathway traveled by the receptors upon PNU-120596 pre-application followed by choline and PNU-120596 co-application.

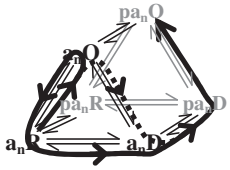

Scheme 3. Proposed predominant pathway traveled by the receptors upon PNU-120596 pre-application followed by choline and PNU-120596 co-application.

In summary, association to open and resting states are probably negligible, and so is the occupancy of PNU-120596-bound resting state (pa$_n$R) itself. This, together with the reasoning for preferring Scheme 4 over Scheme 3 of the accompanying paper (Pesti et al.) gives the following simplified scheme:

3.1.5. *Re-application of agonists*

We have argued that association to resting state must be much slower than to desensitized state. The more important question is, however, whether modulator association to resting receptors occurs at all? (Under *in vivo* conditions, where the modulator would have plenty of time to associate, a mere slowing of association would not make much difference.) The question is not the kinetics, but the equilibrium. We investigated, therefore, the situation when we start from full modulator occupancy (10 μM PNU-120596 co-applied with the agonist), then wash out the agonist while the modulator is continually present, and then test whether dissociation of the modulator occurred by re-application of the agonist. This experiment can be viewed as the combination of the protocols described in Sections 3.1.3 (Fig. 2C) and 3.1.4 (Fig. 3). The initial part is identical with the one shown in Section 3.1.3, but then, the agonist is re-applied and – as it was discussed in Section 3.1.4 – the ratio of modulator-unbound receptors is tested by measuring the magnitude of the first fast current component. Control experiments (as in Fig. 2A) with full washout between agonist-plus-modulator pulses were also done for comparison.

As we have shown in Section 3.1.3, after washing out choline, but keeping PNU-120596 present, the current decayed slowly towards the baseline. The decay is certainly due to the dissociation of the agonist, but what happens with the modulator is uncertain. Modulator molecules may immediately dissociate from agonist-unbound receptors, or they may stay bound to the receptors. If the modulator stayed bound, then upon re-application of the agonist, we would only see agonist-modulated openings, *i.e.*, delayed activation. If, however modulator molecules also dissociated from receptors that had been deserted by agonist molecules, than we would see the re-appearance of the fast first current component (see Section 3.1.4). The magnitude of the fast component, therefore, will reflect how much of the receptors have already lost their modulators.

We used different interpulse intervals (100, 200, 400, 800, 1600, 3200, and 6400 ms), which allowed us to test the magnitude of the fast current component at different times during the decay. An experiment with 1 mM ACh as agonist is shown in Fig. 4A, an example for a control experiment is shown in Fig. 4B. We did not of

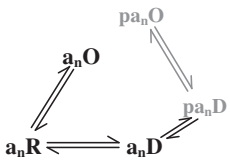

Scheme 4. Minimal model of PNU-120596 action at a single agonist occupancy level.

Please cite this article in press as: Szabo, A.K., et al., Mode of action of the positive modulator PNU-120596 on α7 nicotinic acetylcholine receptors, Neuropharmacology (2014), http://dx.doi.org/10.1016/j.neuropharm.2014.01.033

course expect that the decay of the slow current component will be exactly paralleled by the increase in the fast component, not even in the control case, because after dissociation of either the agonist or the modulator, the receptor needs additional time to recover into resting state. Instead, we compared how the increase of the fast component followed the decay of the slow current, and compared this in control experiments (extracellular solution perfused between pulses) and PNU-120596 unbinding experiments (10 μM PNU-120596 perfused between pulses). Comparison of currents evoked by the first and the second pulse with 3200 ms interpulse interval are shown in Fig. 4C, for 1 mM ACh (left panel), 10 mM ACh (middle panel) and 10 mM choline (right panel). PNU-120596 unbinding experiments are shown in the upper panel, while control experiments in the lower panel. The 3200 ms interpulse interval was chosen for illustration, because at this interval the slow component has not yet decayed to baseline in the case of PNU-120596 unbinding experiments (hence the shifted baseline in Fig. 4C, upper panel), but the fast component is already evident. Dashed lines indicate extrapolation of the slow component to the starting point of the current, to enable measurement of amplitudes in cases when there was a considerable overlap between fast and slow components. We could observe, that in spite of 10 μM of PNU-120596 being continuously present, the fast phase reoccurred with essentially unchanged kinetics. The onset rate of the slow component was significantly increased after prolonged PNU-120596 perfusion. The control onset rate showed considerable variance (ranging from 63 to 719 ms), but PNU-120596 perfusion always significantly accelerated it. For the 6400 ms interpulse interval the 2nd/1st pulse ratio of slow onset time constants was 0.63 ± 0.17, 0.59 ± 0.23 and 0.59 ± 0.16 for 1 mM ACh, 10 mM ACh and 10 mM choline, respectively. The 2nd/1st pulse ratios for control experiments were 0.97 ± 0.08, 0.85 ± 0.09 and 0.97 ± 0.06 for the same agonists. To illustrate how the recovery of the fast component follows the decay of the slow component, we plotted the fractional recovery of the fast component against the fractional decay of the slow component (Fig. 4D). The plots for control *vs.* PNU-120596 experiments were not significantly different with either of the agonists used. This suggests that the rate-limiting step must be agonist dissociation. Once the agonist dissociation has occurred, modulator molecules also rapidly dissociate, and the receptor resumes its agonist-unbound, modulator-unbound resting state relatively rapidly. At the moment we cannot answer the question of how many modulator molecules need to dissociate for the receptor to resume resting state. Recent investigations on PNU-120596-resistant mutants suggest that partially occupied receptors may produce a kinetics similar to that of the modulator-unbound receptor (daCosta and Sine, 2013). The extent of modulator dissociation from all five binding sites may not exactly match the recovery of the fast component, but this does not change our conclusion, that modulator molecules cannot stay bound to agonist-unbound receptors.

3.1.6. *Association of PNU-120596 to different desensitized states*

As we have discussed in the accompanying paper (Pesti et al.), it has been observed in different laboratories, that after prolonged exposure to agonists recovery was more delayed (Uteshev et al., 2002; Wang et al., 2012; Williams et al., 2011a,b), which suggests that more than one desensitized conformational states of α7 nAChR must exist.

We investigated if PNU-120596 had identical effect on different desensitized states. PNU-120596 (10 μM) and choline (10 mM) were co-applied after different durations of 10 mM choline application. Longer durations of pre-exposure to choline caused receptors to progressively enter slow desensitized state. We expected that if either the affinity to separate desensitized states or the efficacy to reactivate receptors from these states is different, then the effect of PNU-120596 would depend on the duration of previous choline exposure. Prolonged choline exposure caused receptors to become progressively less sensitive to the positive modulation by PNU-120596. Fig. 5A illustrates a typical family of currents evoked by choline pre-applications of different durations (15, 95, 175, 335, 655, 1295 and 2575 ms), followed by co-application of PNU-120596

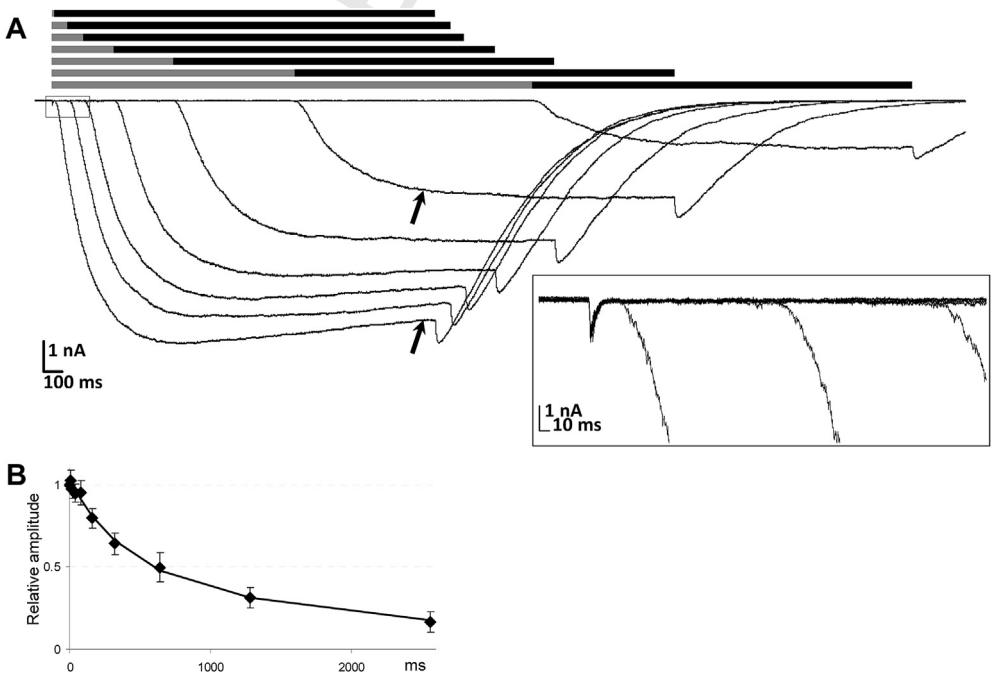

Fig. 5. The effect of PNU 120596 decreased after prolonged choline application. **(A)** Upper panel illustrates the protocol: 10 mM choline (gray bars) and 10 mM choline with 10 μM PNU 120596 (black bars). Choline was applied for 15, 95, 175, 335, 655, 1295 and 2575 ms before co-application of the agonist with the modulator. Inset shows choline-evoked currents at an expanded time scale. Arrows indicate comparison of slow desensitization in the absence and presence of PNU-120596 (see text). **(B)** The time course of the development of insensitivity to PNU 120596 in the presence of 10 mM choline. Black line shows bi-exponential fit to data points.

Please cite this article in press as: Szabo, A.K., et al., Mode of action of the positive modulator PNU-120596 on α7 nicotinic acetylcholine receptors, Neuropharmacology (2014), http://dx.doi.org/10.1016/j.neuropharm.2014.01.033

and choline. Note that the amplitude of the choline-evoked fast current did not change throughout the experiment (see inset). The mean decrease in amplitude (Fig. 5B; amplitudes were measured at the peak of the rebound current component to exclude the effect of channel block) was fit with a biexponential function, the time constants were 353 ms (51% amplitude contribution) and 2379 ms (49% amplitude contribution). Development of a PNU-120596-insensitive desensitized conformation can occur not only in the presence of the agonist alone, but also in the presence of both choline and PNU-120596 (Williams et al., 2011a). In our experiments this could be detected on the first four curves (15–335 ms choline application), where the current started to decay after reaching a maximal amplitude (Fig. 5A). Note however, that in the presence of choline only, the development of this conformation was significantly faster. Compare for example the 1st and 6th traces at ~2 s after the start of agonist application (see arrows in Fig. 5A). In the continuous presence of PNU-120596 (1st trace) the current has only decayed to the 90% of its maximal amplitude, while after a 1295 ms exposure to choline without PNU-120596 (6th trace), the remaining current was 37% of the maximal amplitude.

In summary, our experimental data suggests that PNU-120596 association is most significant to the fast desensitized ("D") states. From our experiments it is not clear whether association to the slow inactivated ("S") states does occur, but the modulator is unable to cause opening, or PNU-120596 cannot even bind to this conformation. If we model the simpler case, where we allow PNU-120596 association only to fast desensitized states, we need to extend Scheme 5 of the accompanying paper (Pesti et al.) with the minimal model of PNU-120596 action. The topology we get is shown in Scheme 5. The model constructed this way can reproduce the characteristic biphasic pattern of currents evoked by choline and PNU-120596 co-application, as well as the concentration- and SXT-dependence of the currents. However, in order to test specific hypotheses regarding the action of PNU-120596, and the interaction between orthosteric and allosteric binding sites, we needed a more complex model.

3.2. Modeling the effect of PNU-120596 on choline-evoked currents

3.2.1. General description of possible models

From the results of experiments we can conclude that the interaction between orthosteric and allosteric ligands is asymmetric. The agonist affects modulator binding indirectly, by causing desensitization. Because PNU-120596 can only associate to desensitized receptors, while dissociates from resting ones, a functional cooperativity emerges. On the other hand, modulator binding seems to affect agonist binding directly, by either increasing the affinity of the orthosteric binding site, or decreasing its accessibility. The former would mean a change in the structure of the binding site, which may accelerate association (which is less likely), slow down dissociation (more likely), or both. Decreased accessibility would mean that both association and dissociation rates are reduced to a similar extent; in essence it means that the modulator can trap agonist molecules in the binding site. The two mechanisms are difficult to tell apart experimentally, therefore we tested in simulations which one offers a plausible explanation for our findings.

In order to address the state-preference of PNU-120596, we needed to extend Scheme 5, by allowing association also to resting and slow desensitized states (Scheme 6). The model thus had a three-dimensional, cubic topology. For the sake of simplicity, we chose to construct a Monod–Wyman–Changeux-type allosteric model. Each agonist binding step contributed equally to the agonist-induced changes in gating rate constants. Another simplification was that – as in the models described above – we still disregarded intermediate occupancy levels of the modulator binding site, and considered only modulator-unbound and modulator-bound states. Introduction of an additional set of modulator-bound closed states ("C1x") was necessary to reproduce single channel bursting behavior. The values of the rate constants, and their calculation are given in Supplementary Table 1. Altogether the model had 54 states, and 212 rate constants, out of which only 16 were free parameters. The rest of the rate constants were calculated using the 8 allosteric factors. In addition, four "symmetrical barrier factors" were introduced in order to be able to test hypotheses regarding binding site accessibility more straightforwardly. Symmetrical barrier factors elevated the energy barrier between two specific sets of states. They did not interfere with detailed balance within the model, because forward and backward rate constants were changed equally (see Supplementary Table 1 for details).

Partitioning of PNU-120596 molecules into/out of the membrane phase seemed to be an essential contributor of current kinetics; therefore we included simulation of accumulation of the

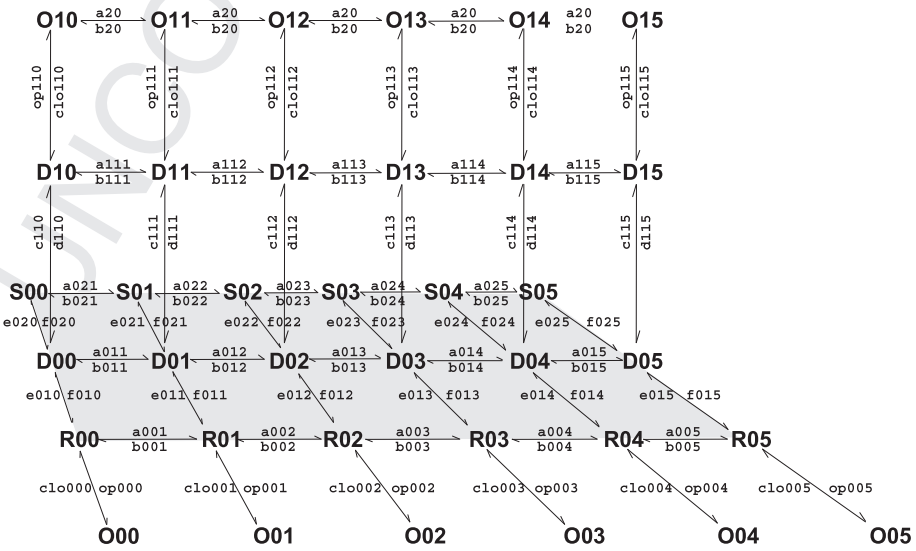

Scheme 5. Minimal model of PNU-120596 action. For the notation of conformational states and rate constants see Scheme 6.

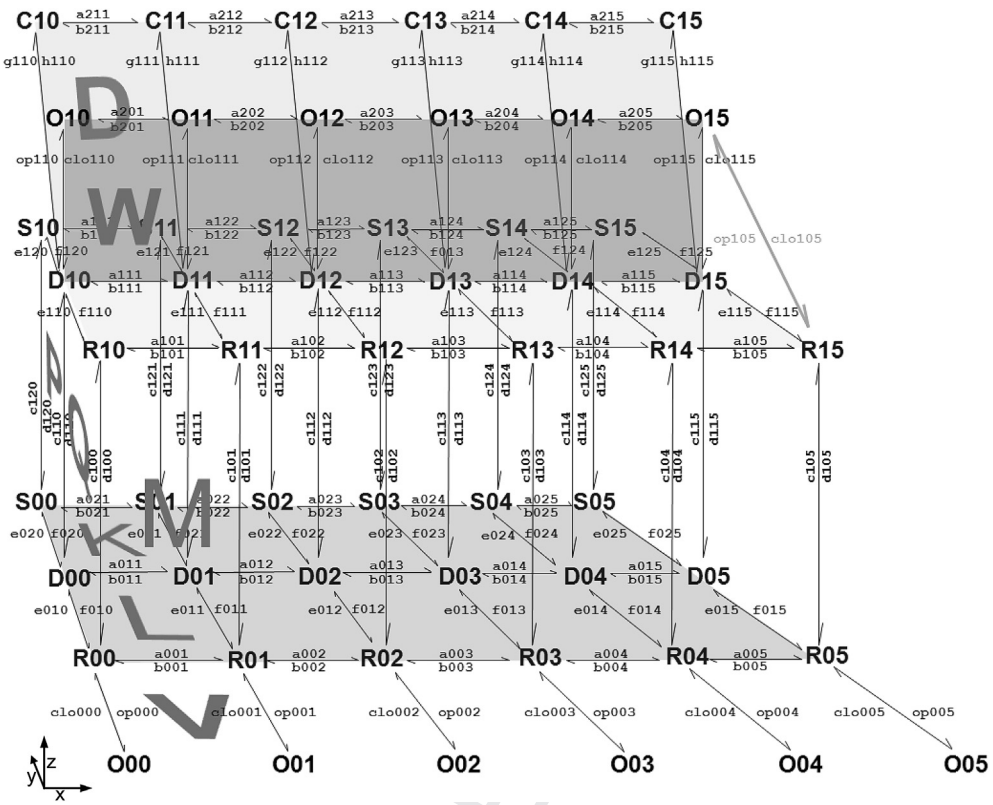

Scheme 6. A Monod–Wyman–Changeux-type cubic model used in our simulations. The states are denoted by a three-character code. The first character indicates the conformation: **O** (open), **R** (resting), **D** (desensitized), **S** (slow desensitized), and **C** (an unknown non-conducting conformation which we needed to suppose – as described below). The second character indicates occupancy of the modulator binding sites (it is either vacant "**0**" or occupied "**1**", and the last character indicates the number of bound agonist molecules from **0** to **5**. Transitions are denoted by a four-character code (except opening and closing transitions) as shown in the figure. The first character, a letter, indicates the nature of transition: "**a**" and "**b**" are association and dissociation of agonist molecules, respectively; "**c**" and "**d**" are association and dissociation of the modulator, **e**, **f**, **g**, **h**, **i**, **j**, **op** (opening) and **clo** (closing) are conformational transitions with no binding/unbinding involved. Only one of the six "**op10x**" "**clo10x**" transitions (modulator-bound resting-open transitions) are shown for clarity (arrow and characters are in gray). The numbers indicate the location of individual transitions within the scheme along the three axes. The first digit indicates presence or absence of PNU-120596 (*z* axis), the second digit indicates the conformation(s) in which, or between which the transition occurs (*y* axis), and the third digit indicates the agonist occupancy level (*x* axis). The allosteric factors **K**, **L**, **V**, **W** and **D** express the interaction between agonist binding and conformational transitions, **P**, and **Q**, between modulator binding and conformational transitions, and **M** expresses cooperativity between agonist and modulator binding. Although the free parameters discussed thus far fully determine all rate constants, it was convenient to introduce some additional factors: they will be called "symmetrical barrier factors", because both forward and backward transitions are to be multiplied by these; in effect they modify the energy barrier of specific transitions. We introduced the following symmetrical barrier factors: **zR**, **zD** and **zS** modifies the rate of PNU-120596 association/dissociation (i.e., transitions along the *z* axis) to states A, B and C states, respectively. The factor **xRDS** modifies the rate of choline association to all PNU-120596-bound states. The additional non-conducting slow-entry-slow-exit states which were required for being able to reproduce burst lengths of modulator-bound receptors were named **C1x** (**C10**–**C15**). These states could be connected to the PNU-120596-bound desensitized states (**D1x** states), the PNU-120596-bound open states (**O1x**), or both. For the sake of simplicity we connected them only to desensitized states.

molecules within the membrane phase. The dynamics of aqueous ($[PNU]_{aq}$) and intramembrane ($[PNU]_{mmb}$) PNU-120596 concentration was simulated using the differential equation:

$$\frac{d[PNU]_{mmb}(t)}{dt} = [PNU]_{aq} * part_{in} - [PNU]_{mmb} * part_{out}$$

where $part_{in}$ and $part_{out}$ are the partitioning rate constants. We do not know the distribution coefficient of PNU-120596 between the membrane and aqueous solution. It is likely that the molecule is accumulated within the membrane phase, because it is a lipophilic molecule, but partitioning and distribution coefficients (log*P* and log*D*) are only estimated for the water–octanol distribution, which can be much different from the membrane–aqueous phase distribution. We chose the membrane–aqueous solution distribution coefficient to be 1 (supposing ten-fold accumulation).

We first confirmed that partitioning of the modulator can account for the acceleration of the current onset upon pre-incubation in PNU-120596 as described in Section 3.1.4. We tested how the receptors would behave if affinity of the modulator was insensitive to receptor conformation (parameter set "A" in Table 1). Association

Table 1
The values of allosteric factors and symmetrical barrier factors in parameter sets "A" to "D".

	A	B	C	D
Q	1	0.15	0.15	0.15
M	1	1	2.1	1.25
xRDS	1	1	0.01	0.001

Allosteric factor **Q** quantifies the interaction between modulator binding and desensitization. **Q** < 1 indicates that modulator-bound receptors favor desensitized state, and that the modulator has higher affinity to desensitized receptors. Allosteric factor ***M*** indicates the cooperativity between the agonist and the modulator. Values >1 indicate that binding of one ligand increases affinity of the other binding site. Symmetrical barrier factor: **xRDS** <1 indicates an increased energy barrier for modulator-bound receptors (all conformations) along the ***x*** axis *i.e.*, it slows down agonist association and dissociation equally.
The parameter sets: **A)** basic model; no effect of the modulator on the resting – desensitized equilibrium, no cooperativity between agonist and modulator binding sites, both agonist and modulator association is unhindered. **B)** The modulator favors the desensitized state. **C)** Higher cooperativity, and moderately hindered accessibility of the agonist binding site. **D)** Moderate cooperativity, and a strongly hindered accessibility of the agonist binding site.

to resting conformation was also possible in this case, and as expected, we observed a depletion of the first fast current component (Fig. 6A, upper panel). We attempted to reproduce currents as shown in Fig. 3 by modifying the affinity to resting conformation. We did this by modifying the allosteric factor "Q" (see Scheme 6). Decreasing "Q" slows down the association of the modulator, with leaving the dissociation unaltered, while this modification is balanced by promoting modulator-bound desensitization. To achieve an extent of decrease in the first current component that matches data obtained in experiments (9.4%), we needed to decrease Q at least to 0.15 (parameter set "B"), which corresponds with association to resting conformation 44.4-fold slower (Fig. 6A lower panel). The same extent of decrease in affinity was also required to reproduce the magnitude of the fast current component in re-application experiments, as it was shown in Section 3.1.5.

3.2.2. Simulation of the decay phase

As it has been shown in Section 3.1.3, when the agonist was washed out in the continuing presence of the modulator, the decay was slowed by almost an order of magnitude. The reason for this, as we have mentioned, can either be that modulator binding increases the affinity of the orthosteric binding site, or that it "traps" agonist molecules within the binding site. We tested both mechanisms in simulations.

When association and dissociation rates of agonist molecules were independent of modulator binding, the decay was inappropriate, much faster than in experiments (Fig. 6B, parameter set "B").

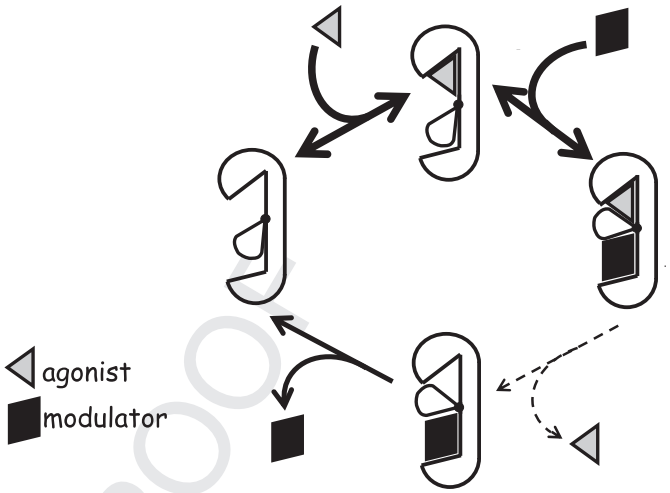

Fig. 7. Schematic drawing illustrating the mechanism of interaction between agonist and PNU-120596 (see text for explanation).

The allosteric factor *M* (see Scheme 6) indicated the cooperative interaction between agonist and modulator affinity. Introducing cooperativity by elevating this factor only, did not prove sufficient to reproduce the slowed decay. On the other hand, hindered accessibility of the agonist in modulator-bound receptors also was

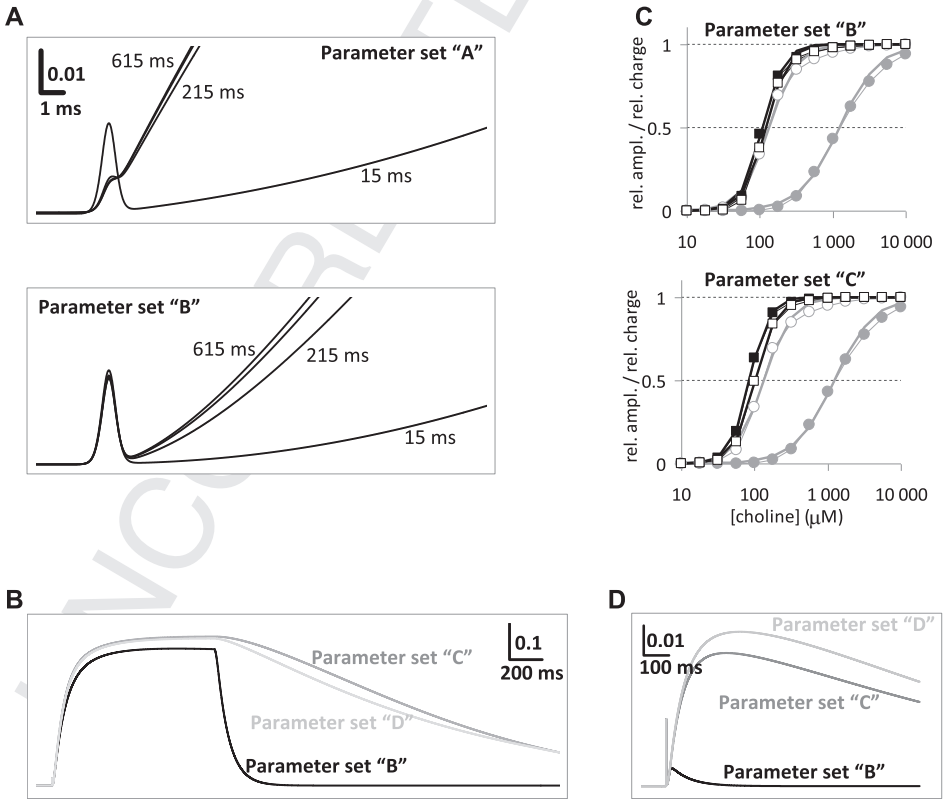

Fig. 6. Dependence of simulated current properties on specific parameters. Simulations of currents show the occupancy of all open states as a function of time. **(A)** PNU-120596 association to resting state. The four traces show the initial part of simulated currents after 15, 215, 415 and 615 ms of 10 μM PNU-120596 pre-incubation. Upper and lower panels show simulations with parameter sets (see Table 1), "A" (equal association rate to resting and desensitized states) and "B" (decreased association to resting state, balanced by favored desensitized conformation upon modulator binding), respectively. **(B)** Choline dissociation from modulator-bound receptors. The simulated currents were evoked by a 1 s co-application of choline and PNU-120596, followed by a 2 s application of PNU-120596, using three parameter sets (see Table 1). **(C)** Concentration–relative amplitude (filled symbols) and concentration–relative net charge (open symbols) plots in the presence of 10 μM PNU-120596, for two parameter sets. Plots for modulator–free agonist evoked currents are shown in gray. Thick lines show fits of the Hill equation to data points. **(D)** The first second of simulated 10 mM choline evoked currents when the behavior of the model was investigated under more physiological circumstances: short (10 ms) pulses of the agonist at a continuous presence of a lower concentration of PNU-120596 (1 μM).

Please cite this article in press as: Szabo, A.K., et al., Mode of action of the positive modulator PNU-120596 on α7 nicotinic acetylcholine receptors, Neuropharmacology (2014), http://dx.doi.org/10.1016/j.neuropharm.2014.01.033

insufficient in itself. (Hindered accessibility was achieved by introducing the symmetrical barrier factor xRDS, i.e., by decreasing both association and dissociation rate constants equally.) However, when the two modifications were introduced in parallel, the slow decay rate was reproduced. Strongly hindered accessibility (xRDS = 0.001) required only weak cooperativity: $M = 1.25$ (this means that the affinity of choline was increased $1.25^2 = 1.56$-fold by modulator binding), while even a strong cooperativity ($M > 2$) required radically restricted accessibility (e.g., $M = 2.1$ and xRDS = ~0.01; $M = 4.9$ and xRDS = 0.05). Simulations with two combinations of M a xRDS are shown in Fig. 6B. The shape of the curve (immediate exponential decay upon agonist removal) was better reproduced by parameter set "D" (weak cooperativity, strongly hindered access). A few other parameters also affected the decay rate, but the single essential requirement was obviously decreased agonist dissociation from modulator-bound receptors. Both M and xRDS parameters affected agonist dissociation; the extent of decrease is given by M^2/xRDS. We can calculate, therefore, that modulator-bound receptors had to have a 400–4000-fold slower agonist dissociation than modulator-free receptors in all parameter sets which reproduced the extent of decay found in experiments. We propose that in the presence of PNU-120596, the ability of choline to dissociate from its binding site is radically reduced. This may be accompanied with a moderately increased affinity for the agonist (i.e., cooperativity between orthosteric and allosteric binding sites), but based on the simulations, hindered accessibility, not increased affinity seems to be the predominant mechanism.

We tested the concentration–response behavior of the model in the total absence of cooperativity ($M = 1$; parameter set "B"). Fig. 6C (upper panel) illustrates concentration–amplitude and concentration–net charge flux (area under curve; AUC) curves for choline from simulated currents evoked in the presence of 10 μM PNU 120596. Concentration–response curves in the absence of PNU-120596 (from Fig. 8B of the accompanying paper) are also shown in gray color for comparison. As we have shown there, the EC_{50} values for unmodulated currents were 1.24 mM and 135 μM for peak amplitude and AUC, respectively (AUC calculated from the first 200 ms). With choline and 10 μM PNU-120596 co-applied, the EC_{50} values were 109 μM (amplitude; $n_H = 3.01$) and 121 μM (AUC; $n_H = 2.92$). This means that for current amplitudes a 11.3-fold apparent increase in choline affinity was observed even in the "no-cooperativity" model (i.e., when there was no change in microscopic agonist affinity). For the AUC plots the increase in apparent affinity was minimal (1.11-fold). This clearly shows that an apparent increase in affinity can occur without binding of one ligand actually affecting the affinity of the other binding site. Introducing cooperativity ($M = 2.1$, parameter set "C") did not cause a large shift in the concentration response curve (Fig. 6C, lower panel), the EC_{50} values were 85.5 μM (amplitude; $n_H = 3.30$) and 102.5 μM (AUC; $n_H = 3.01$). Although parameter set "D" imposed a 4.41-fold higher microscopic affinity on the model than parameter set "C", it only caused a 1.28-fold increase in macroscopic affinity. In fact, compared to the huge difference between the concentration–peak amplitude and the concentration–AUC curves, the effect of PNU-120596 on the AUC curves seems negligible even with parameter set "D", which caused the largest shift of the curves. The reason for this, we believe, is the specific property of the α7 nAChR, i.e., that maximal efficacy in terms of net charge flux is already reached at submaximal agonist occupancy (Mike et al., 2000; Papke et al., 2000). The concentration–peak amplitude curve keeps increasing even after reaching maximal net charge flux, but higher agonist concentrations merely cause faster transfer of the same amount of ions. We might phrase it this way: The increase in apparent affinity caused by PNU-120596 merely unmasked the characteristic concentration–net charge flux relationship of the α7 nAChR. A genuine increase in agonist affinity upon modulator binding might have been present, but it probably only had a minor effect on concentration–response curves.

While the effect of the modulator on the EC_{50} (affinity) of the agonist was questionable, its effect on amplitudes (efficacy) was obvious. Thus far we have considered agonist affinity only; which means studying relative amplitudes and relative charge fluxes. In terms of absolute net charge flux, the effect of PNU-120596 is enormous, and the differences between parameter sets are also great. Fig. 6D illustrates the importance of the hindered agonist dissociation in a quasi-physiological situation with lower PNU-120596 concentration (1 μM aqueous concentration), and a short (10 ms) agonist pulse (10 mM choline). We simulated the case when the modulator had sufficient time beforehand to accumulate within the membrane phase. The difference between unhindered (parameter sets "A" and "B"), and hindered (parameter sets "C" and "D") agonist dissociation models was considerable. The extent of increase in charge flux calculated over a 1 s period during and after a 10 ms pulse of 10 mM choline was for unhindered agonist dissociation parameter sets 110.8 ("A") and 31.2 ("B") times the charge carried by the current evoked by choline alone, while for hindered agonist dissociation sets it was much higher: 2392 ("C") and 2001 ("D"). This also indicates that a hindered agonist dissociation form modulator-bound receptors is a fundamental element of the mechanism.

3.3. Summary of the mechanism of PNU-120596 on α7 nAChRs

The two major observations regarding the mechanism of the interaction between the agonist and the modulator are based on the experiments described in Sections 3.1.3, 3.1.4, and 3.1.5, and on the analysis by simulations in Sections 3.2.1 and 3.2.2: (1) Dissociation of the agonist is hindered from modulator-bound receptors. (2) Affinity of PNU-120596 to resting state is low. Let us consider what follows from these observations in a physiological situation, where there is an ambient level of the modulator, and the agonist is released in pulses. The essence of the mechanism is illustrated on a schematic drawing (Fig. 7).

Before the agonist pulse, the vacant receptor cannot bind the modulator, because it has low affinity to resting conformation. Once the agonist pulse has started, the agonist can immediately bind to the easily accessible modulator-unbound receptor. It causes the receptor to desensitize, thereby providing access for the modulator. Modulator binding induces a set of conformational states, which causes agonist dissociation to slow down radically; in effect modulator binding traps the agonist in its binding site. Once the agonist has ultimately dissociated, the cycle is completed by modulator dissociation, which allows the receptor to resume its original resting state. Note that the agonist association is fast, because it predominantly occurs to the highly accessible conformation of the orthosteric site, but agonist dissociation is slow, because it predominantly occurs from a low-accessibility site.

The trapped agonist cycle mechanism seems to be a requirement for type II PAM action, as we have seen from simulations with parameter sets "B" to "D". Without introducing decreased agonist accessibility, the current had only a minor delayed component after the agonist had been removed (Fig. 6D).

4. Conclusions

We investigated the mechanism of modulation of α7 nAChR function by PNU-120596 in experiments, and tested various hypotheses for possible mechanisms by kinetic simulations. Our major conclusions are as follows:

Please cite this article in press as: Szabo, A.K., et al., Mode of action of the positive modulator PNU-120596 on α7 nicotinic acetylcholine receptors, Neuropharmacology (2014), http://dx.doi.org/10.1016/j.neuropharm.2014.01.033

The current evoked by choline in the presence of PNU-120596 was biphasic. The first phase had a fast onset and decay, and it reflected unmodulated choline-evoked current. The onset of the first phase was essentially unchanged even when PNU-120596 was pre-applied, although in this case the fast decay of the first phase could not be seen, because the two phases partially merged.

The unchanged fast onset suggested that association to resting channels was hindered. Kinetic modeling suggested that affinity to resting conformation must be at least 44-fold lower than to desensitized state. We propose, that when receptors are activated by agonist–modulator co-application, they typically desensitize before they bind modulator molecules.

Application of PNU-120596 after prolonged (several seconds long) choline perfusion evoked currents with decreased amplitude. This confirms the existence of PNU-120596-insensitive slow desensitized state(s). We observed that gating into PNU-120596-insensitive desensitized states was faster in the absence of the modulator.

The interaction of the agonist and modulator revealed that dissociation of choline molecules was radically hindered by bound modulator molecules. In kinetic simulations agonist dissociation had to be at least ~400- to 4000-fold slower from modulator-bound receptors to reproduce experimentally observed decay rates.

The large apparent increase in agonist affinity upon PNU-120596 binding in simulations did not require actual cooperativity between agonist and modulator binding sites on the level of rate constants, i.e., modification of microscopic affinity (although it also did not exclude it). Experimental current forms were best reproduced by a very week cooperativity.

We propose an explanation for type II PAM mechanism of action, based upon two critical observations: i) choline dissociation from PNU-120596-bound channels is hindered, and ii) PNU-120596 affinity to resting channels is low. We propose, that even in the continuous presence of the modulator, its association is minimal, because the receptors are in resting state. Whenever the concentration of the agonist is increased, a cycle of events occurs: the agonist binds to an unhindered binding site, and desensitizes the receptor, the modulator can bind to desensitized conformation, and it induces a set of conformational states, in which opening of the pore is energetically more favorable, and in which the agonist is kept trapped in its binding site. This produces a prolonged period of intense activity, when the effect of the agonist is both prolonged and enhanced (i.e., the open probability is increased). Once the agonist has finally dissociated, the modulator also dissociates, and the cycle is terminated. The requirements for this "trapped agonist cycle" mechanism are the following: The receptor needs to have two ligands with a specific type of interaction: Binding of "ligand A" (the agonist in this case) must increase the accessibility of "ligand B" (the modulator), while binding of "ligand B" must decrease the accessibility of "ligand A". The mechanism does not require that the orthosteric and allosteric ligands actually modify each other's microscopic affinity. In situations, where the agonist comes in short pulses (as it is probably the case for *in vivo* receptors) and only the modulator is present continually, this mechanism provides an exceptionally effective way of enhancing the signal.

Acknowledgment

The pCEP4/rat α7 nAChR expressing GH4C1 cell line was kindly provided by Siena Biotech S.p.A. (Siena, Italy). This work was supported by grant NK72959 from the Hungarian Research Fund (OTKA) and by the Project Based Personnel Exchange Program of the Hungarian Scholarship Board (MÖB) and the German Academic Exchange Service (DAAD).

Appendix A. Supplementary data

Supplementary data related to this article can be found at http://dx.doi.org/10.1016/j.neuropharm.2014.01.033.

References

AhnAllen, C.G., 2012. The role of the alpha7 nicotinic receptor in cognitive processing of persons with schizophrenia. Curr. Opin. Psychiatry 25, 103–108.
Bouzat, C., Bartos, M., Corradi, J., Sine, S.M., 2008. The interface between extracellular and transmembrane domains of homomeric Cys-loop receptors governs open-channel lifetime and rate of desensitization. J. Neurosci. 28, 7808–7819.
Costa, R., Motta, E.M., Manjavachi, M.N., Cola, M., Calixto, J.B., 2012. Activation of the alpha-7 nicotinic acetylcholine receptor (alpha7 nAchR) reverses referred mechanical hyperalgesia induced by colonic inflammation in mice. Neuropharmacology 63, 798–805.
daCosta, C.J., Free, C.R., Corradi, J., Bouzat, C., Sine, S.M., 2011. Single-channel and structural foundations of neuronal α7 acetylcholine receptor potentiation. J. Neurosci. 31, 13870–13879.
daCosta, C.J., Sine, S.M., 2013. Stoichiometry for drug potentiation of a pentameric ion channel. Proc. Natl. Acad. Sci. U. S. A. 110, 6595–6600.
Faghih, R., Gfesser, G.A., Gopalakrishnan, M., 2007. Advances in the discovery of novel positive allosteric modulators of the alpha7 nicotinic acetylcholine receptor. Recent Pat. CNS Drug. Discov. 2, 99–106.
Faghih, R., Gopalakrishnan, M., Briggs, C.A., 2008. Allosteric modulators of the alpha7 nicotinic acetylcholine receptor. J. Med. Chem. 51, 701–712.
Freitas, K., Carroll, F.I., Damaj, M.I., 2013. The antinociceptive effects of nicotinic receptors alpha7-positive allosteric modulators in murine acute and tonic pain models. J. Pharmacol. Exp. Ther. 344, 264–275.
Friis, S., Mathes, C., Sunesen, M., Bowlby, M.R., Dunlop, J., 2009. Characterization of compounds on nicotinic acetylcholine receptor alpha7 channels using higher throughput electrophysiology. J. Neurosci. Methods 177, 142–148.
Gronlien, J.H., Hakerud, M., Ween, H., Thorin-Hagene, K., Briggs, C.A., Gopalakrishnan, M., Malysz, J., 2007. Distinct profiles of alpha7 nAChR positive allosteric modulation revealed by structurally diverse chemotypes. Mol. Pharmacol. 72, 715–724.
Hurst, R.S., Hajos, M., Raggenbass, M., Wall, T.M., Higdon, N.R., Lawson, J.A., Rutherford-Root, K.L., Berkenpas, M.B., Hoffmann, W.E., Piotrowski, D.W., Groppi, V.E., Allaman, G., Ogier, R., Bertrand, S., Bertrand, D., Arneric, S.P., 2005. A novel positive allosteric modulator of the alpha7 neuronal nicotinic acetylcholine receptor: in vitro and in vivo characterization. J. Neurosci. 25, 4396–4405.
Isaacson, M.D., Horenstein, N.A., Stokes, C., Kem, W.R., Papke, R.L., 2013. Point-to-point ligand-receptor interactions across the subunit interface modulate the induction and stabilization of conformational states of alpha7 nAChR by benzylidene anabaseines. Biochem. Pharmacol.. Q2
Jindrichova, M., Lansdell, S.J., Millar, N.S., 2012. Changes in temperature have opposing effects on current amplitude in alpha7 and alpha4beta2 nicotinic acetylcholine receptors. PLoS One 7, e32073.
Li, F., Chen, Z., Pan, Q., Fu, S., Lin, F., Ren, H., Han, H., Billiar, T.R., Sun, F., Li, Q., 2013. The protective effect of PNU-282987, a selective alpha7 nicotinic acetylcholine receptor agonist, on the hepatic ischemia-reperfusion injury is associated with the inhibition of high-mobility group box 1 protein expression and nuclear factor kappaB activation in mice. Shock 39, 197–203.
Liu, C., Su, D., 2012. Nicotinic acetylcholine receptor alpha7 subunit: a novel therapeutic target for cardiovascular diseases. Front. Med. 6, 35–40.
Malysz, J., Gronlien, J.H., Anderson, D.J., Hakerud, M., Thorin-Hagene, K., Ween, H., Wetterstrand, C., Briggs, C.A., Faghih, R., Bunnelle, W.H., Gopalakrishnan, M., 2009a. In vitro pharmacological characterization of a novel allosteric modulator of alpha 7 neuronal acetylcholine receptor, 4-(5-(4-chlorophenyl)-2-methyl-3-propionyl-1H-pyrrol-1-yl)benzenesulfonami de (A-867744), exhibiting unique pharmacological profile. J. Pharmacol. Exp. Ther. 330, 257–267.
Malysz, J., Gronlien, J.H., Timmermann, D.B., Hakerud, M., Thorin-Hagene, K., Ween, H., Trumbull, J.D., Xiong, Y., Briggs, C.A., Ahring, P.K., Dyhring, T., Gopalakrishnan, M., 2009b. Evaluation of alpha7 nicotinic acetylcholine receptor agonists and positive allosteric modulators using the parallel oocyte electrophysiology test station. Assay. Drug. Dev. Technol. 7, 374–390.
Mazurov, A.A., Speake, J.D., Yohannes, D., 2012. Discovery and development of alpha7 nicotinic acetylcholine receptor modulators. J. Med. Chem. 54, 7943–7961.
Mike, A., Castro, N.G., Albuquerque, E.X., 2000. Choline and acetylcholine have similar kinetic properties of activation and desensitization on the alpha7 nicotinic receptors in rat hippocampal neurons. Brain Res. 882, 155–168.
Milescu, L.S., Nicolai, C., Bannen, J., 2000-2013. QuB Software.
Papke, R.L., Kem, W.R., Soti, F., Lopez-Hernandez, G.Y., Horenstein, N.A., 2009. Activation and desensitization of nicotinic alpha7-type acetylcholine receptors by benzylidene anabaseines and nicotine. J. Pharmacol. Exp. Ther. 329, 791–807.
Papke, R.L., Meyer, E., Nutter, T., Uteshev, V.V., 2000. alpha7 receptor-selective agonists and modes of alpha7 receptor activation. Eur. J. Pharmacol. 393, 179–195.
Papke, R.L., Thinschmidt, J.S., 1998. The correction of alpha7 nicotinic acetylcholine receptor concentration–response relationships in Xenopus oocytes. Neurosci. Lett. 256, 163–166.

Please cite this article in press as: Szabo, A.K., et al., Mode of action of the positive modulator PNU-120596 on α7 nicotinic acetylcholine receptors, Neuropharmacology (2014), http://dx.doi.org/10.1016/j.neuropharm.2014.01.033

Pesti, K., Szabo, A.K., Mike, A., Vizi, E.S. Kinetic properties and open probability of α7 nicotinic acetylcholine receptors. Neuropharmacology.

Russo, P., Taly, A., 2012. alpha7-Nicotinic acetylcholine receptors: an old actor for new different roles. Curr. Drug. Targets 13, 574–578.

Sitzia, F., Brown, J.T., Randall, A.D., Dunlop, J., 2011. Voltage- and temperature-dependent allosteric modulation of alpha7 nicotinic receptors by PNU120596. Front. Pharmacol. 2, 81.

Uteshev, V.V., Meyer, E.M., Papke, R.L., 2002. Activation and inhibition of native neuronal alpha-bungarotoxin-sensitive nicotinic ACh receptors. Brain Res. 948, 33–46.

Vizi, E.S., Fekete, A., Karoly, R., Mike, A., 2010. Non-synaptic receptors and transporters involved in brain functions and targets of drug treatment. Br. J. Pharmacol. 160, 785–809.

Wang, J., Papke, R.L., Stokes, C., Horenstein, N.A., 2012. Potential state-selective hydrogen bond formation can modulate activation and desensitization of the alpha7 nicotinic acetylcholine receptor. J. Biol. Chem. 287, 21957–21969.

Williams, D.K., Peng, C., Kimbrell, M.R., Papke, R.L., 2012. Intrinsically low open probability of alpha7 nicotinic acetylcholine receptors can be overcome by positive allosteric modulation and serum factors leading to the generation of excitotoxic currents at physiological temperatures. Mol. Pharmacol. 82, 746–759.

Williams, D.K., Wang, J., Papke, R.L., 2011a. Investigation of the molecular mechanism of the Alpha7 nAChR positive allosteric modulator PNU-120596 provides evidence for two distinct desensitized states. Mol. Pharmacol..

Williams, D.K., Wang, J., Papke, R.L., 2011b. Positive allosteric modulators as an approach to nicotinic acetylcholine receptor-targeted therapeutics: advantages and limitations. Biochem. Pharmacol..

Xiong, J., Yuan, Y.J., Xue, F.S., Wang, Q., Cheng, Y., Li, R.P., Liao, X., Liu, J.H., 2012. Postconditioning with alpha7 nAChR agonist attenuates systemic inflammatory response to myocardial ischemia-reperfusion injury in rats. Inflammation 35, 1357–1364.

Young, G.T., Zwart, R., Walker, A.S., Sher, E., Millar, N.S., 2008. Potentiation of alpha7 nicotinic acetylcholine receptors via an allosteric transmembrane site. Proc. Natl. Acad. Sci. U. S. A. 105, 14686–14691.

Please cite this article in press as: Szabo, A.K., et al., Mode of action of the positive modulator PNU-120596 on α7 nicotinic acetylcholine receptors, Neuropharmacology (2014), http://dx.doi.org/10.1016/j.neuropharm.2014.01.033